

REVISTA AIDIS

de Ingeniería y Ciencias Ambientales:
Investigación, desarrollo y práctica.

BIOCHAR FROM ANDROPOGON GRASS (*Andropogon gayanus* cv. *Planaltina*) APPLICATIONS IN DYE REMOVAL BY ADSORPTION AND SLOW FILTRATION

Cleidiane Cardoso Teixeira¹

Argemiro Lima Pedrosa²

Iago Aguiar Dias Carmo³

Marcelo Mendes Pedroza²

Nelson Luis Gonçalves Dias de Souza³

* Grasielle Soares Cavallini³

Recibido el 17 de septiembre de 2021. Aceptado el 21 de febrero de 2022

Abstract

Dyes represent a class of contaminants with a high impact on aquatic ecosystems due to their toxicity. As these pollutants are difficult to degrade, studies on the treatment methods for these compounds are highly important to minimize damage to water bodies that receive these effluents. In this work, the adsorption and slow filtration processes using charcoal produced from the pyrolysis of Andropogon grass (*Andropogon gayanus* cv. *Planaltina*) were individually evaluated for removal of the methylene blue dye. The adsorption studies included the evaluation of kinetic behavior, evaluating pseudo-first-order and pseudo-second-order models and adsorption isotherms using the Langmuir, Freundlich, and Dubinin-Radushkevich models. According to the results, it was found that the adsorptive process had greater efficiency between pH 8 and 10. The pseudo-second-order model better described the adsorption kinetic behavior ($R^2 = 0.9722$) and as for the adsorption isotherms, Freundlich's model best described the process. The maximum charcoal adsorption capacity of Andropogon grass for the removal of methylene blue was 17.63 mgg^{-1} . In the filtration process, dye removal reached an efficiency above 99% at filtration rates of 1.5 and 2.1 $\text{m}^3\text{m}^{-2}\text{day}^{-1}$.

Keywords: biomaterial, bioadsorbent, dye, filtration, adsorption.

¹ Colegiado de Ciências Exatas e Biotecnológicas, Universidade Federal do Tocantins, Brasil.

² Instituto Federal do Tocantins, Brasil.

³ Programade Pós-Graduação em Química, Universidade Federal do Tocantins, Brasil.

Corresponding author: Federal University of Tocantins - Undergraduate Programme in Chemistry, 77.402-970, Gurupi, Tocantins, Brazil. Email: grasielesoares@gmail.com; grasiele@uft.edu.br

Introduction

Dyes used in textile industries are manufactured in such a way that they are resistant to exposure to light, water, soap, perspiration, chemical substances, and microbial attacks, which makes them persistent in the environment (Chandra, 2016). In industrial effluents, dyes are among the most polluting contaminants (Resta *et al.*, 2016; Yaseen and Scholz, 2019), as even in a small fraction they can promote impacts such as changes in gas solubility and water transparency, in addition, they are hardly removed by conventional effluent treatments due to their complex composition (Zazycki *et al.*, 2019).

The removal of these dyes from water bodies is extremely important as they are considered a risk to public health because most of these substances present toxicity and carcinogenic potential (Hassaan and El Nemr, 2017). As for the impacts on ecosystems, the presence of dyes in an aqueous medium can present toxicity to the biota, as well as reduce the passage of light preventing the photosynthesis process (Holkar *et al.*, 2016; Rosa *et al.*, 2019).

Due to the specificity of each dye, there is no standardization as to the most suitable treatment method for its removal, with the most commonly used conventional methods being: chemical precipitation, ozonization, electro-flocculation, chemical coagulation, oxidation, biological treatment, ultrafiltration, electrochemical treatment, ion exchange, membrane filtration and adsorption (Choudhary *et al.*, 2020; Tomczyk *et al.*, 2020).

Adsorption technologies are highlighted, as they are effective in the treatment of industrial effluents regarding the removal of metals and dyes (Ms and Hasan, 2016). According to Baccar *et al.* (2009) activated carbon has been widely used in the treatment of water and effluents, due to its high adsorption capacity, but depending on the source of the raw material, such as wood, lignite, and mineral coals, the cost of its production is high (Baccar *et al.*, 2009). In this context, there is great interest in the use of low-cost alternative materials that can be used in the production of charcoal, such as coconut husks, peat, petroleum residues, rice husks, walnuts, animal bones, grains, coffee, peach, plum, and almond pits (Wu *et al.*, 2019). Which can originate from forest species, industrial, urban, and agricultural residues, among others. According to Dalahmeh *et al.*, 2012, the high surface area of charcoal of vegetable origin offers a high capacity for removing organic matter by adsorption and by biofilm (Dalahmeh *et al.*, 2012).

Fast-growing plants such as grasses also have the potential for biochar production. Specifically, Andropogon grass was used for metal removal in the after-treatment of paint industry effluent, and removals greater than 97% were obtained for total aluminum, total cadmium, hexavalent chromium, zinc, and total cobalt, in addition to removal of 92% color (Pedrosa *et al.*, 2019).

According to Embrapa Cerrados, *Andropogon* grass (*Andropogon gayanus* cv. Planaltina) is a perennial forage grass originally from Tropical Africa and was widely distributed in most tropical Cerrados, as it presents areas of dry seasons and prolonged periods. The cultivar of the *Andropogon gayanus* Kunt species was the first tropical forage launched in 1980, however, it has been showing a behavior with a strong tendency to occupy non-cultivated environments close to the plantation areas. The Planaltina cultivar has the following characteristics: adaptation to sandy or gravel soils, acid and of low natural fertility; presents rapid regrowth at the beginning of the rains; has fire tolerance; high compatibility with herbaceous forage legumes; and lower food value during the dry season. This cultivar stands out for its high resistance to leafhoppers from pastures, and also for showing excellent adaptation to restrictive soil and climate conditions (Andrade *et al.*, 1980).

In this context, the present study evaluated the retention capacity of the methylene blue dye through adsorption and slow filtration processes, using a filter built on a laboratory scale, using charcoal obtained from the process of pyrolysis of the biomass of *Andropogon* grass. The physicochemical characteristics of coal were evaluated by Raman and Infrared spectroscopy.

Materials and methods

Biochar production from *Andropogon* grass

The biomass of *Andropogon* grass was collected in Palmas, Tocantins, Brazil (S10°22'32.5" W48°18'15.7"). To obtain the fiber, the grass was crushed in a knife mill and crushed again in a blender, then the biomass was subjected to drying at 40 °C for 24 hours and then sieved. The material retained between the 28 and 48 mesh sieves was mixed and used for the characterization and production of charcoal.

The biochar was produced by the slow pyrolysis process in a stainless steel bipartite fixed bed reactor, 100 cm long and 10 cm external diameter, brand FLYEVER, model FE50RPN, 05/50 line, with a microcontroller coupled to a reclining oven, tubular up to 1200 °C and 1 zone. The biomass (dry mass of 64.74g) was introduced into the reactor tube in the form of briquettes. The pyrolysis reactor coupled to a thermocouple was initially heated to an oven temperature of 200 °C. Then, the temperature of the device was increased according to the operating conditions of the pyrolysis process, which ranged from 400 °C to 500 °C, for 30 minutes. The flow rate of the carrier gas (nitrogen) was 3mLmin⁻¹. Pedrosa *et al.* (2019) characterized this biomaterial as mesoporous, with moisture content 9.9% ± 0.1, ash content 4.5% ± 0.3, apparent density 0.824 mg L⁻¹ and pH 8.9.

Adsorptive studies using charcoal from *Andropogon* grass to remove methylene blue

A 5.12 mgL⁻¹ solution of methylene blue was used to carry out the tests at different pH values: 2, 4, 6, 8, 10 and 12. Adjustments of the pH values of the methylene blue solutions were performed with solutions of sulfuric acid (0.1 molL⁻¹) and sodium hydroxide (0.1 molL⁻¹), using a pH meter

(MS Tecnopon®), with the samples under agitation. In a glass flask with a lid, 0.01 g of the charcoal from Andropogon grass was weighed, then 20 mL of each methylene blue solution was added. The samples were left under agitation for 15 hours. The methylene blue removal efficiency was evaluated by visible spectrophotometry in a PG instruments model T60 UV-Vis spectrophotometer. Absorbance measurements were performed at a wavelength of 664 nm. The amount of methylene blue adsorbed by the adsorbent at each pH value was calculated by the following Equation 1:

$$Q_e = \frac{(C_0 - C_e)V}{m} \quad \text{Equation (1)}$$

Where: Q_e is the amount of dye adsorbed by the adsorbent, C_0 (mgL^{-1}) and C_e (mgL^{-1}) correspond to the initial concentrations and final equilibrium concentration of the dye, m is the mass of the adsorbent and V is the volume of the dye solution in contact with the adsorbent. The adsorption rate was calculated by Equation 2:

$$\% \text{ removal} = \frac{(C_0 - C_e)}{C_0} * 100 \quad \text{Equation (2)}$$

Adsorption isotherms were calculated from the following concentrations: 40.96 mgL^{-1} , 30.72 mgL^{-1} , 20.48 mgL^{-1} , 10.24 mgL^{-1} and 5.12 mgL^{-1} . In a glass flask with a lid, 0.01 g of the charcoal from Andropogon grass was weighed, then 20 mL of each methylene blue solution was added. The samples were left under agitation for 24 h. The data obtained were adjusted to Langmuir, Freundlich, Dubinin-Radushkevich and Redlich–Peterson isotherms.

For the kinetic assay, a methylene blue concentration of 5.12 mgL^{-1} was used. For this, a glass flask with a lid was used, in which 0.1 g of the biochar from Andropogon grass was weighed, then 250 mL of the methylene blue solution was added. The system was agitated for 24 h and aliquots to evaluate the adsorption of the dye concerning time were collected over time. The kinetic behavior of the adsorptive process was evaluated according to two pseudo-first-order and pseudo-second-order models.

Filtration using biochar from Andropogon grass to remove methylene blue

The particle size characterization of the charcoal filter was determined by the effective diameter and the uniformity coefficient (CU) of the filter media. The effective diameter being defined as the opening of the sieve that allows the accumulated passage of 10% of the analyzed sample. And the uniformity coefficient is the porosity of the sieve that retains 40% of the sample divided by the effective diameter (Bourke *et al.*, 1995; Sheng, 2007; Munk *et al.*, 2017)

The test was carried out on a laboratory scale, in a descending filter containing the charcoal produced by the pyrolysis of Andropogon grass as a filtering medium. The experiment was carried out in continuous flow, using the methylene blue solution at a concentration of 20.01 mgL^{-1} at pH 7.0. Two filters of equal dimensions were used: total height of the filter tubing with connections of 25 cm, height of the carbon layer in the tubing of 10 cm and filter diameter of 1.9 cm in each filter. During the assembly of the system, the mass of 3.984 grams of coal was used. Filters were fed by gravity, and two filtration rates were evaluated, $1.5 \text{ m}^3\text{m}^{-2}\text{day}^{-1}$ and $2.1 \text{ m}^3\text{m}^{-2}\text{day}^{-1}$.

Dye retention was measured in a double-beam spectrophotometer (PERKIN ELMER, LAMBDA 750) at 650 nm, using a calibration curve with R^2 equal to 0.9991, constructed by solutions with concentrations of 1.0; 5.0; 10.0; 15.0 and 24.0 mgL^{-1} .

Raman spectroscopy

Raman spectra were performed on an RFS 100 instrument (Bruker, Ettlingen, Germany), equipped with a $\text{Nd}^{+3}/\text{YAG}$ laser operating at 1064 nm with a Ge detector cooled with liquid nitrogen and with a spectral resolution of 4 cm^{-1} and 1024 accumulations were performed with a laser power of 60 mW. For the calculation of the ratio of the D and G bands intensities, it is important to clearly define a protocol for the exclusion of the baseline, necessary to access the spectroscopic information. The procedure used was the exclusion of a linear baseline between 1000 and 1900 cm^{-1} using a spline function and multiple points. To adjust the spectrum, the Gauss function was used for the D and G bands, resulting in an $R^2 = 0.97$.

Infrared absorption spectroscopy

The infrared spectra of the samples were obtained in a Perkin Elmer brand FTIR spectrometer in the region of $4000\text{-}400 \text{ cm}^{-1}$, with a resolution of 4 cm^{-1} and an average of 64 scans.

Results and discussion

Spectroscopic evaluation of the biomaterial

The biomaterial was analyzed using Raman and Infrared vibrational spectroscopic methods to characterize its chemical structure. Figure 1 shows the Raman spectrum of biochar and it is possible to observe two characteristic bands of carbonic material, one at 1272 cm^{-1} (D band) and the other at 1592 cm^{-1} (G band) (Cuesta *et al.*, 1994; Sheng, 2007; Munk *et al.*, 2017). Both reveal the presence of sp^2 -type hybridization carbon atoms in benzene or partially hydrogenated condensed benzene rings (Fuertes *et al.*, 2010).

The D band is characteristic of polyaromatic carbons and can be attributed to the vibration mode of the graphitic network with A_{1g} symmetry, and its relative intensity and width vary according to the disorder or defect of the material (Keown Li, Hayashi Li, 2007; Sadezky *et al.*, 2005). The G

band corresponds to an ordered graphite network and can be attributed to the vibration mode of the double bonds between carbon atoms and the vibration of the graphite network with E_{2g} symmetry (Chen *et al.*, 2015; Hoslett *et al.*, 2020). The curve fitting of the Raman spectrum is widely used for the analysis of the biochar structure, and the methods that use only the G and D bands are simpler. Methods using five to ten bands are also described in the literature, however, in this work, only the D and G band was used because it is a single material (Tsaneva *et al.*, 2014; Pusceddu, 2017; Wang *et al.*, 2018; Yu *et al.*, 2018).

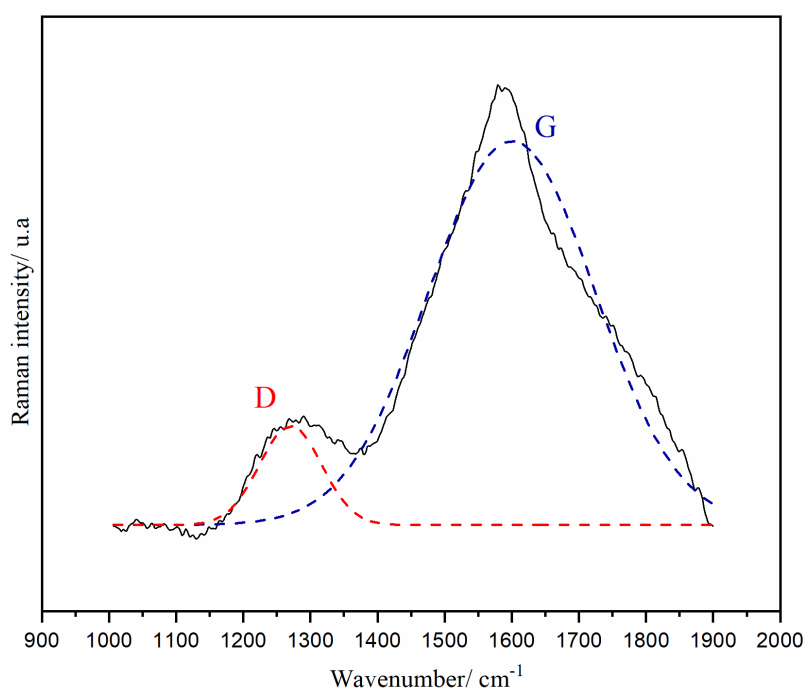


Figure 1. Biochar Raman spectrum obtained by pyrolysis of Andropogon grass.

The band intensities ratio (I_D/I_G) is an important qualitative parameter to assess the structure of materials, indicating the level of disorder and defect in the material. A ratio greater than 1 indicates an interruption in sp^2 hybridization due to a large number of defects and a ratio lower than 1 is characteristic of material with fewer structural defects and a better graphitic network (Genovese *et al.*, 2015; Mendonça *et al.*, 2017; Eshun *et al.*, 2019). The calculated ratio for the obtained biochar was 0.26; which indicates a structure with fewer defects and better structural organization. This value can be associated with the low temperature used for pyrolysis (450°C) and a low ash content ($13.23 \pm 0.63\%$) since high carbonization and biochar temperatures with lower ash contents generate graphite with crystallites more disorderly and amorphous. In addition, Raman spectroscopy can be

used to measure the average size of carbon crystallite in the (La) plane. This is done by taking the G-bandwidth value at half height (Γ_G) and using a mathematical equation built from Raman spectroscopy and X-ray diffraction data.. Thus, in the Raman spectrum of the biochar $\Gamma_G = 292 \text{ cm}^{-1}$, is observed, which gives an average crystallite size of 1.99 nm.

Figure 2 shows the infrared absorption spectrum of biochar before and after the filtration process with the methylene blue solution.

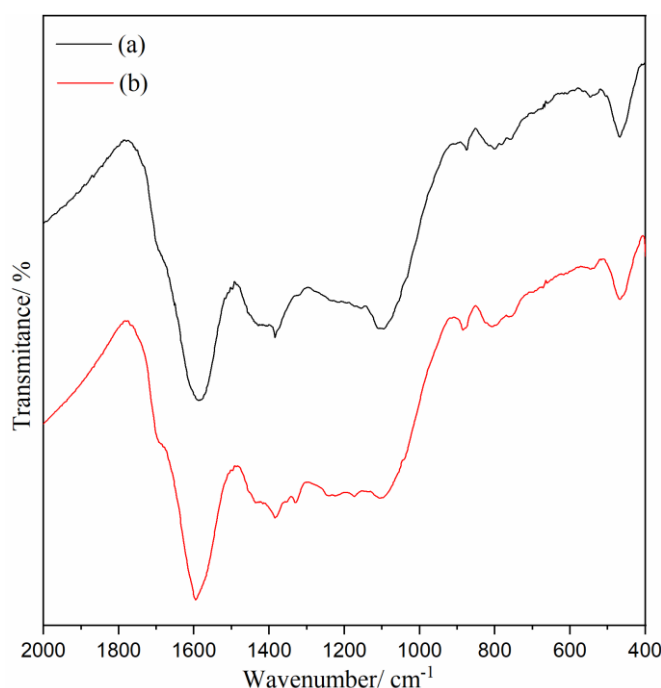


Figure 2. The infrared spectrum of biochar was obtained from the pyrolysis of Andropogon grass before (a) and after (b) the adsorption of the methylene blue dye.

Comparing the spectra, no spectral changes are observed in the bands in 3391, 2965/2925/2854, 1688, 1434 e 468 cm^{-1} , assigned respectively to the $\nu(\text{OH})$, $\nu(\text{CH}_2)$, $\nu(\text{C}=\text{O})$, $\nu(\text{CH})$ and $\nu(\text{CH})$ and aromatic compounds. However, small spectral changes are observed in other regions of the spectrum. The bands on 1584 e 875 cm^{-1} , which can be assigned respectively to the $\nu(\text{C}=\text{C})$ e $\nu(\text{CH})$ aromatic, are respectively shifted to 1594 and 783 cm^{-1} in the spectrum of the biochar with the dye. In addition, there is an increase in the relative intensity of the bands in 1384 and 1328, assigned respectively to the $\nu(\text{C}-\text{C})$ in aromatics and $\nu(\text{C}-\text{O})$ in phenols and decreased relative intensity of the band in 1099 cm^{-1} that can be attributed to the $\nu(\text{C}-\text{O}-\text{C})$ (Chia *et al.*, 2012; Mupa *et al.*, 2016; Zhu *et al.*, 2018; Fazal *et al.*, 2019) . Thus, from the results obtained by infrared spectroscopy, it can be

inferred that the adsorption that occurs is not chemical, as for this to occur, more significant spectral changes would be necessary as described in the literature (Liu *et al.*, 2020; Suwunwong *et al.*, 2020). Mainly in the bands referring to C=C/C=O and OH bonds, which would indicate respectively π - π type interactions and hydrogen bonds.

Evaluation of pH in the adsorption of methylene blue on Andropogon grass biochar

The results of the evaluation of the adsorptive process at different pH values are shown in Table 1.

Table 1. Adsorption values at different pH.

pH	Qe (mg/g)	% Removal
2	5.1991	53
4	6.4649	66
6	6.1677	63
8	7.72504	79
10	7.1847	73
12	4.6984	48

The pH that presented the lowest removal rate was pH = 2, this may occur because methylene blue is a cationic molecule, so at more acidic pH values there may be competition between the H_3O^+ ions and the dye, reducing the efficiency of the adsorptive process (Shee *et al.*, 2014). The results showed that the best working range is between pH 8 and 10, with a removal percentage of 79 and 73%, respectively.

Adsorption Isotherm

The isotherms used to describe the adsorption process using Andropogon grass and methylene blue dye were: Langmuir, Freundlich, Dubinin-Radushkevich and Redlich–Peterson. Figure 3 presents the models, the equations provided and the coefficient of determination (R^2). To interpret the data, the parameters of each model were calculated, which are shown in Table 2

The values of R^2 shown in Figure 3 demonstrate that the Langmuir ($R^2 = 0.9748$) and Freundlich ($R^2 = 0.9765$) models fitted very well to the experimental data by the linear regression method because the coefficient of determination R^2 presented values close to a 1, which indicates good applicability in both isotherm models. However, the Dubinin-Radushkevich and Redlich–Peterson models, despite having presented a lower R^2 than the previous ones, still presents a good fit, which allows use the first them to calculate the average adsorption energy (E).

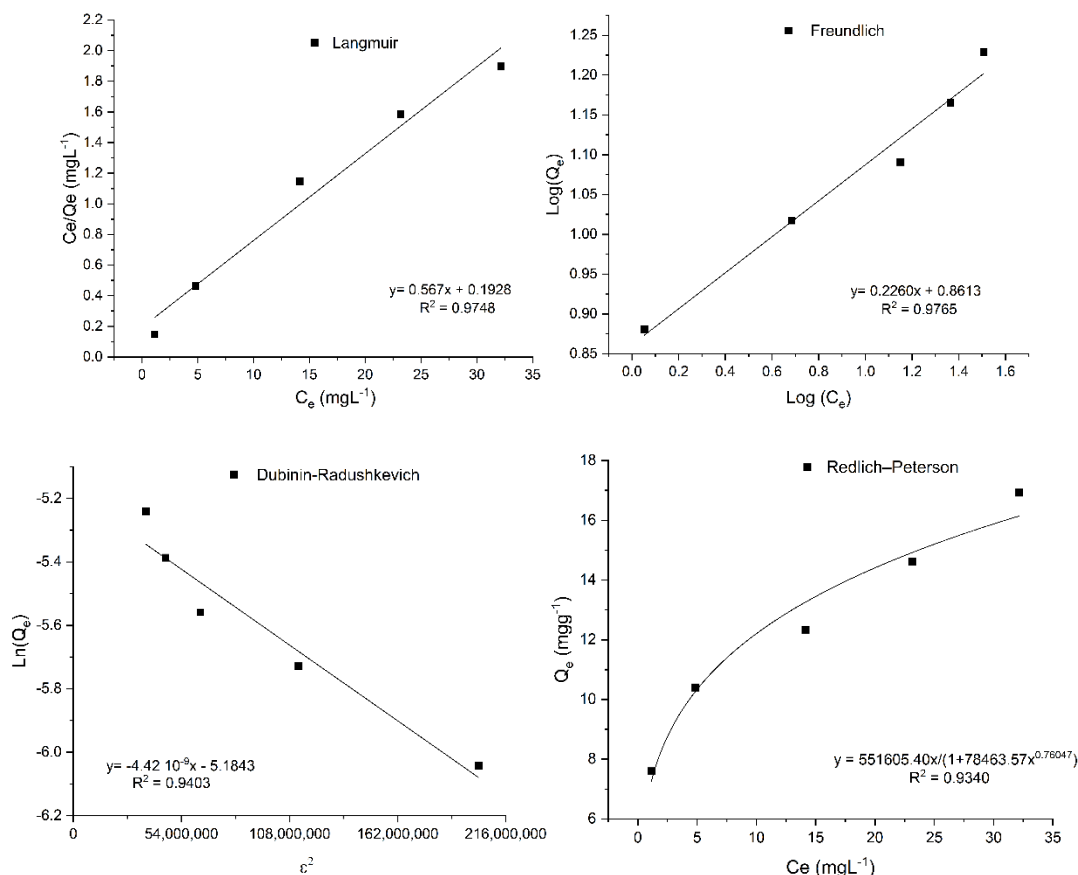


Figure 3. Langmuir, Freundlich and Dubinin-Radushkevich isotherms.

Table 2. Langmuir, Freundlich and Dubinin-Radushkevich isotherm parameters.

Langmuir	Freundlich	Dubinin-Radushkevich	Redlich-Peterson
$Q_{max} \text{ (mgg}^{-1}\text{)} = 17.63$			$K_R \text{ (Lmg}^{-1}\text{)} = 551605.40$
$K_L \text{ (Lmg}^{-1}\text{)} = 0.294$	$K_F \text{ (mgg}^{-1}\text{)} = 2.366$		$A_R \text{ (Lmg}^{-1}\text{)} = 78463.57$
$R_L = 0.0767$	$n \text{ (mgL}^{-1}\text{)} = 4.424$	$E \text{ (kJmol}^{-1}\text{)} = 1.063$	$\beta = 0.76047$

The Langmuir isotherm assumes that the adsorption sites are energetically identical, that the adsorbent has a uniform surface and the adsorption takes place in a monolayer. From this model, it is possible to obtain the maximum adsorption capacity (Q_{max}) and the parameter R_L , which indicates whether the Langmuir isotherm is favorable, unfavorable, linear, or irreversible. A favorable isotherm will achieve high solid loading values even at low adsorbate values in the fluid

phase, unlike an unfavorable isotherm. In the linear isotherm, the loading will increase linearly with the concentration of the solution, and in the irreversible, it will present a very strong interaction, so the adsorbed amount is independent of its concentration in the fluid (Ayawei *et al.*, 2017). Being, $R_L > 1$ when the process was unfavorable, $R_L = 1$ for linear isotherm, R_L between 0 e 1 when the process is favorable and $R_L = 0$ when the process is irreversible (Crini and Badot, 2008). The value of (Q_{max}) of Andropogon grass biomass for methylene blue removal according to the Langmuir model was 17.63 mgg^{-1} . The value of R_L obtained was 0.0767 which indicates favorable adsorption, as its value was between 0 and 1.

The Freundlich model considers that the solid is constituted by several different types of active sites and that its surface is heterogeneous, therefore it does not assume adsorption only in a monolayer. From this model, it is possible to obtain the K_F (adsorption capacity) and n (adsorption intensity), which represent the adsorption capacity and the distribution of the adsorption sites in terms of their energy, respectively. Thus, when the value of K_F is between 1 and 20 mgg^{-1} , the adsorption is feasible, when $n = 1$, the partition between the two phases is independent of the concentration, if $1/n < 1$, normal adsorption occurs, if $1/n > 1$ suggests cooperative adsorption and when n is a value between 1 and 10, the adsorption process is favorable (Komkiene and Baltreinaite, 2016; Ayawei *et al.*, 2017; Shikuku and Jemutai-Kimosop, 2020; Iqbal *et al.*, 2021). In the present work, the K_F value was 2.366 mgg^{-1} , indicating the capacity of Andropogon grass biochar to adsorb the dye. The value of n was 4.424 mgL^{-1} , therefore, the adsorption process is favorable and normal. The Freundlich model is the most used to describe the adsorption characteristic of coal used for the treatment of water and effluents (Metcalf *et al.*, 2002).

The Redlich-Peterson isothermal model combines Langmuir elements and Freundlich equations, and the adsorption mechanism is a unique hybrid and does not follow the ideal monolayer adsorption. It can be applied in homogeneous and heterogeneous systems, due to its versatility. From this model it is possible to obtain the parameters k_R and a_R (constants of the isotherm) and β , a dimensionless parameter of the model that varies from 0 to 1. When $\beta = 0$ the equation obtained is similar to the Freundlich equation. When $\beta = 1$, the equation resembles that of Langmuir (Tosun *et al.*, 2012).

Finally, the Dubinin-Radushkevich isotherm is an adsorption model generally applied to express adsorption mechanism with Gaussian energy distribution on heterogeneous surfaces. The model is a semi-empirical equation in which adsorption follows a pore-filling mechanism. From this model, it is possible to differentiate physical (physisorption) and chemical (chemisorption) adsorption by obtaining the average adsorption energy. Thus, if physisorption occurs, the average adsorption energy has a value between 1 and 8 kJmol^{-1} , while if there is chemisorption (ion exchange) the energy value must have a value between $8-16 \text{ kJmol}^{-1}$ (Bertolini *et al.*, 2013; Ayawei *et al.*, 2017).

The Andropogon grass biochar presented average adsorption energy of 1.063 kJmol^{-1} , thus indicating that the adsorption process is physical, which corroborates the result obtained using infrared spectroscopy.

Adsorption Kinetics

The kinetics of the methylene blue adsorption process was investigated by applying pseudo-first-order and pseudo-second-order linear kinetic models, to study the mechanism that controls the kinetic process and find the time in which the adsorbent/dye equilibrium occurs. Figure 4 shows the linear fit of the data to the models and the adsorption kinetic parameters obtained by the linearization of the data are presented in Table 3.

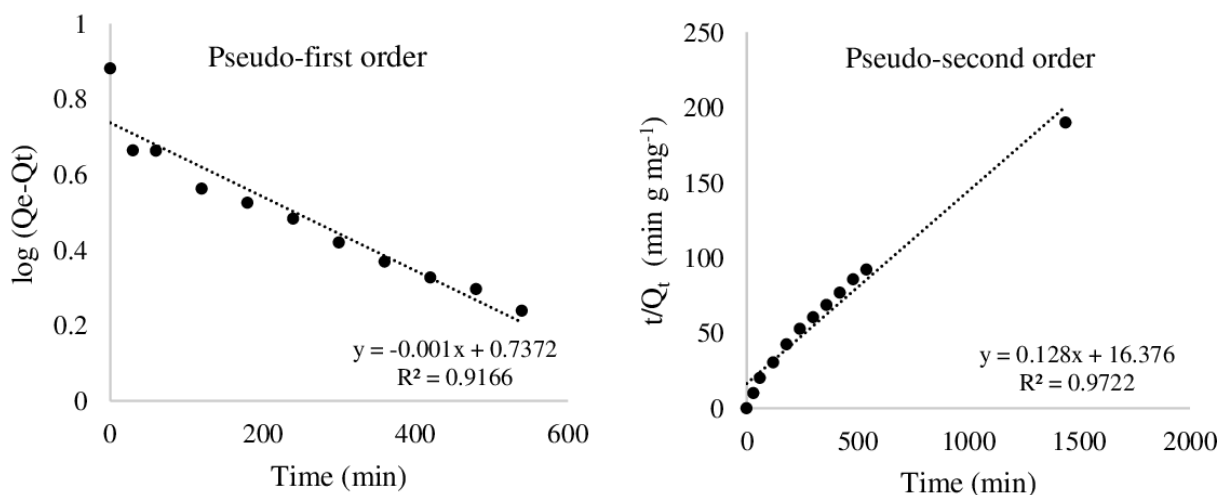


Figure 4. Pseudo-first order and Pseudo-second order kinetic models.

Table 3. Kinetic parameters of pseudo-first-order and pseudo-second-order models.

Model	Parameters	Values
Pseudo-first order	k_1	$2.303 \times 10^{-3} \text{ min}^{-1}$
Pseudo-second order	k_2	$1.001 \times 10^{-3} \text{ gmg}^{-1} \text{ min}^{-1}$

Analyzing the data obtained, it appears that the pseudo-second-order model better described the adsorption kinetics, as the value of R^2 was closer to 1. This model indicates that the adsorption rate depends on the adsorption capacity of the material and not on the adsorbate concentration. From this model it is also possible to calculate the theoretical value of Q_e , which was 7.8125 mgg^{-1} , very close to the experimental value of 7.5824 mgg^{-1} (Sahoo and Prelot, 2020).

Efficiency of the filtration process using methylene blue solution

The filter removal efficiency was evaluated at two filtration rates $1.5 \text{ m}^3\text{m}^{-2}\text{day}^{-1}$ and $2.1 \text{ m}^3\text{m}^{-2}\text{day}^{-1}$, both corresponding to a slow filtration. The filter was operated until the saturation of the filter medium, which was verified by the decline in the filtration rate and the reduction in filter efficiency, as shown in Figure 5.

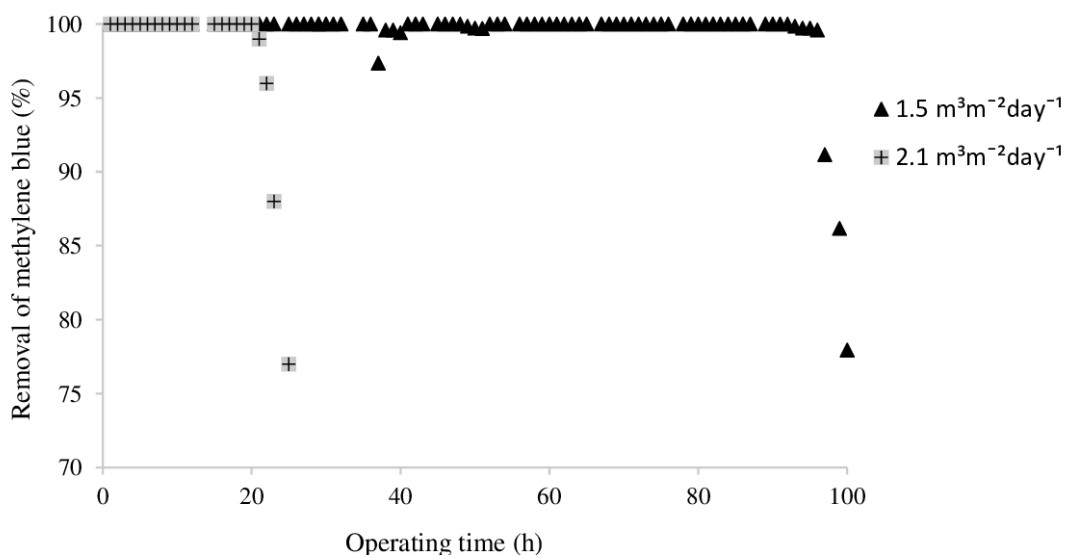


Figure 5. Filtration of methylene blue in biochar obtained by pyrolysis of Andropogon grass.

For a filtration rate of $1.5 \text{ m}^3\text{m}^{-2}\text{day}^{-1}$, the total dye retention persisted for 92 hours, corresponding to 1.65 liters of the filtered sample. After this period, there was the transfer of the dye, which indicates that the adsorption capacity of the biochar begins to be depleted (Metcalf *et al.*, 2002). For the rate of $2.1 \text{ m}^3\text{m}^{-2}\text{day}^{-1}$, the operating time until filter saturation was 22 hours, equivalent to 0.66 liters of the filtered sample. To avoid filter clogging, it is necessary to balance the hydraulic and organic load of the liquid and the properties of the filter medium (Torrens *et al.*, 2009), that is why the study of filtration at different rates is important for the process.

Considering the volume treated in the first 22 hours, the rate of $1.5 \text{ m}^3\text{m}^{-2}\text{day}^{-1}$ had a yield 4 times lower, however, the lower cleaning frequency is an advantage compared to the rate of $2.1 \text{ m}^3\text{m}^{-2}\text{day}^{-1}$. According to the characterization of the biomaterial, infrared spectroscopy showed that the adsorption of the dye occurred physically. This behavior is consistent with the structure with few defects observed by the Raman spectrum, as this characteristic makes it less reactive and therefore chemical adsorption did not occur.

It is noteworthy that in addition to the adsorption capacity, the filter removal efficiency depends on the porosity, the specific surface area, the reactivity, and the ability to promote the development of films. (Rolland *et al.*, 2009). Pedrosa *et al.*, (2019) described this biomaterial as mesoporous but did not evaluate its adsorbent potential (Pedrosa *et al.*, 2019). Regarding the reactivity with the filtering medium and the dye in, a low reactivity can be observed, which can be explained by the little significant change in the infrared spectrum.

The effective diameter obtained by the granulometric analysis of the Andropogon grass biochar was 0.3 mm, and the uniformity coefficient corresponded to 2. Both values are within the range indicated by the Water Treatment Manual for a slow filtration, which must fall between 0.25 - 0.35 mm of effect diameter and uniformity coefficient less than 3, featuring a filter medium with uniform particles that allow a filtration process with retention in deeper regions of the filter, and thus greater use of the filter medium (Bourke *et al.*, 1995).

Conclusions

The adsorption studies carried out with the biomass of Andropogon grass demonstrated that this biochar could adsorb the methylene blue dye, which is favored when performed in pH ranges between 8 and 10.

As for the adsorption isotherms, all models were satisfactory, however, the models that had the best fit were Freundlich and Langmuir, as they presented similar coefficients of determination and closer to 1. According to the Langmuir model, the maximum adsorption capacity of biochar of Andropogon grass for the removal of methylene blue dye was 17.63 mgg^{-1} and from a favorable process. The Freundlich isotherm indicated a favorable process and normal adsorption, and the Dubinin-Radushkevich isotherm described the adsorption process as physical.

The methylene blue adsorption kinetics on the study carbon showed that the pseudo-second-order model was the best fit model, presenting a theoretical Q_e value very close to the experimental one.

The slow filtration tests showed that the biochar produced from the pyrolysis of Andropogon grass has a high capacity to retain the methylene blue dye. Both filtration rates demonstrated dye removal efficiency, however, the rate of $2.1 \text{ m}^3\text{m}^{-2}\text{day}^{-1}$ would require much downtime due to the need to clean the filter.

As for the characterization of the biomaterial, it was possible to observe using Raman spectroscopy that the material has a more ordered structure and few defects, which makes it less

reactive and not susceptible to chemical adsorption. Finally, infrared spectroscopy allowed us to characterize the chemical structure of the material and determine the occurrence of physical adsorption of methylene blue in the biochar.

Acknowledgments

The authors would like to thank CAPES (Coordenação de Aperfeiçoamento de Pessoal de Nível Superior - Coordination for the Improvement of Higher Education Personnel - Brazil) (Financing Code 001 CAPES). This work was carried out with the support of the National Council for Scientific and Technological Development – CNPq – Brazil; Federal University of Tocantins (UFT) for financial assistance (PROPESQ).

References

- Andrade, R.P., Sanzonowicz, C., Gomes, D.T., Rocha, C.M.C.D., Couto, W., Thomas, D., MOORE, C.P. (1980) Preliminary recommendations for the formation of Andropogon Planaltina grass pastures. Planaltina: EMBRAPA-CPAC, 1-3.
- Ayawei, N., Ebelegi, A.N., Wankasi, D. (2017) Modelling and Interpretation of Adsorption Isotherms. *Journal of Chemistry*, **2017**, 1-11. <https://doi.org/10.1155/2017/3039817>
- Baccar, R., Bouzid, J., Feki, M., Montiel, A. (2009) Preparation of activated carbon from Tunisian olive-waste cakes and its application for adsorption of heavy metal ions. *J. Hazard. Mater.*, **162**, 1522-1529. <https://doi.org/10.1016/j.jhazmat.2008.06.041>
- Bertolini, T.C.R., Izidoro, J.C., Magdalena, C.P., Fungaro, D.A. (2013) Adsorption of Crystal Violet Dye from Aqueous Solution onto Zeolites from Coal Fly and Bottom Ashes. *Orbital: Electron. J. Chem.*, **5**, 179-191.
- Bourke, N., Carty, G., Crowe, M., Lambert, M. (1995) Water treatment manuals: filtration. Environmental Protection Agency Irlanda.
- Chandra, R. (2016) Environmental Waste Management. CRC Press. <https://doi.org/10.1201/b19243>
- Chen, W., Chen, M., Zhou, X. (2015) Characterization of Biochar Obtained by Co-Pyrolysis of Waste Newspaper with High-Density Polyethylene. *Bioresources*. <https://doi.org/10.15376/biores.10.4.8253-8267>
- Chia, C.H., Gong, B., Joseph, S.D., Marjo, C.E., Munroe, P., Rich, A.M. (2012) Imaging of mineral-enriched biochar by FTIR, Raman and SEM-EDX. *Vib. Spectrosc.*, **62**, 248-257. <https://doi.org/10.1016/j.vibspec.2012.06.006>
- Choudhary, M., Kumar, R., Neogi, S. (2020) Activated biochar derived from Opuntia ficus-indica for the efficient adsorption of malachite green dye, Cu⁺² and Ni⁺² from water. *J. Hazard. Mater.*, **392**, 122441. <https://doi.org/10.1016/j.jhazmat.2020.122441>
- Crini, G., Badot, P.-M. (2008) Application of chitosan, a natural aminopolysaccharide, for dye removal from aqueous solutions by adsorption processes using batch studies: A review of recent literature. *Progress in Polymer Science*, **33**, 399-447. <https://doi.org/10.1016/j.progpolymsci.2007.11.001>
- Cuesta, A., Dhamelincourt, P., Laureyns, J., Martínez-Alonso, A., Tascón, J.M.D. (1994) Raman microprobe studies on carbon materials. *Carbon*, **32**, 1523-1532. [https://doi.org/10.1016/0008-6223\(94\)90148-1](https://doi.org/10.1016/0008-6223(94)90148-1)
- Dalahmeh, S.S., Pell, M., Vinnerås, B., Hylander, L.D., Öborn, I., Jönsson, H. (2012). Efficiency of Bark, Activated Charcoal, Foam and Sand Filters in Reducing Pollutants from Greywater. *Water Air Soil Pollut.*, **223**, 3657-3671. <https://doi.org/10.1007/s11270-012-1139-z>

- Eshun, J., Wang, L., Ansah, E., Shahbazi, A., Schimmel, K., Kabadi, V., Aravamudhan, S. (2019) Characterization of the physicochemical and structural evolution of biomass particles during combined pyrolysis and CO₂ gasification. *J. energy Inst.*, **92**, 82-93. <https://doi.org/10.1016/j.joei.2017.11.003>
- Fazal, T., Faisal, A., Mushtaq, A., Hafeez, A., Javed, F., Alaud Din, A., Rashid, N., Aslam, M., Rehman, M.S.U., Rehman, F. (2019) Macroalgae and coal-based biochar as a sustainable bioresource reuse for treatment of textile wastewater. *Biomass Convers. Biorefin.*, <https://doi.org/10.1007/s13399-019-00555-6>
- Fuertes, A.B., Camps Arbestain, M., Sevilla, M., Maciá-Agulló, J., Fiol, S., López, R., Smernik, R., Aitkenhead, W., Arce, F., Macias, F. (2010) Chemical and structural properties of carbonaceous products obtained by pyrolysis and hydrothermal carbonisation of corn stover. *Aust. J. Soil Res.*, **48**, 618-626. <https://doi.org/10.1071/SR10010>
- Genovese, M., Jiang, J., Lian, K., Holm, N. (2015) High capacitive performance of exfoliated biochar nanosheets from biomass waste corn cob. *J. Mater. Chem. A*, **3**, 2903-2913. <https://doi.org/10.1039/C4TA06110A>
- Hassaan, M., El Nembr, A. (2017) Health and Environmental Impacts of Dyes: Mini Review. *Am. J. Environ. Sci.*, **1**, 64-67. <https://doi.org/10.11648/j.ajese.20170103.11>
- Holkar, C.R., Jadhav, A.J., Pinjari, D.V., Mahamuni, N.M., Pandit, A.B. (2016) A critical review on textile wastewater treatments: Possible approaches. *J. environ. Manage.*, **182**, 351-366. <https://doi.org/10.1016/j.jenvman.2016.07.090>
- Hoslett, J., Ghazal, H., Mohamad, N., Jouhara, H. (2020) Removal of methylene blue from aqueous solutions by biochar prepared from the pyrolysis of mixed municipal discarded material. *Sci. total environ.*, **714**, 136832. <https://doi.org/10.1016/j.scitotenv.2020.136832>
- Iqbal, T., Iqbal, S., Batool, F., Thomas, D., Iqbal, M.M.H. (2021) Utilization of a Newly Developed Nanomaterial Based on Loading of Biochar with Hematite for the Removal of Cadmium Ions from Aqueous Media. *Sustainability*, **13**, 2191. <https://doi.org/10.3390/su13042191>
- Komkiene, J., Baltreinaite, E. (2016) Biochar as adsorbent for removal of heavy metal ions [Cadmium(II), Copper(II), Lead(II), Zinc(II)] from aqueous phase. *Int. J. new Technol. Res.*, **13**, 471-482. 1 <https://doi.org/10.1007/s13762-015-0873-3>
- Liu, L., Deng, G., Shi, X. (2020) Adsorption characteristics and mechanism of p-nitrophenol by pine sawdust biochar samples produced at different pyrolysis temperatures. *Sci. Rep.*, **10**, 5149. <https://doi.org/10.1038/s41598-020-62059-y>
- Mendonça, F.G.d., Cunha, I.T.d., Soares, R.R., Tristão, J.C., Lago, R.M. (2017) Tuning the surface properties of biochar by thermal treatment. *Bioresour. Technol.*, **246**, 28-33. <https://doi.org/10.1016/j.biortech.2017.07.099>
- Metcalf, Eddy, I., Tchobanoglous, G., Burton, F., Stensel, H.D. (2002) Wastewater Engineering: Treatment and Reuse. McGraw-Hill Education.
- Ms, A., Hasan, A. (2016) Removal of Heavy Metals from Industrial Waste Water by Biomass-Based Materials: A Review. *J. Ind. Pollut. Control*, **5**, 1-13. <https://doi.org/10.4172/2375-4397.1000180>
- Munk, M., de Souza Salomão Zanette, R., de Almeida Camargo, L.S., de Souza, N.L.G.D., de Almeida, C.G., Gern, J.C., de Sa Guimaraes, A., Ladeira, L.O., de Oliveira, L.F.C., de Mello Brandão, H. (2017) Using carbon nanotubes to deliver genes to hard-to-transfect mammalian primary fibroblast cells. *Biomed. Phys. Eng. Express.*, **3**, 045002. <https://doi.org/10.1088/2057-1976/aa7927>
- Mupa, M., Rutsito, D., Musekiwa, C. (2016) Removal of methylene blue from aqueous solutions using biochar prepared from Eichhornia crassipes (Water Hyacinth)-molasses composite: Kinetic and equilibrium studies. *Afr. J. Pure Appl. Chem.*, **10**, 63-72. <https://doi.org/10.5897/AJPAC2016.0703>
- Pedrosa, A.L., Pedroza, M.M., Cavallini, G.S. (2019) Post-treatment of paint industry effluents by filtration using Andropogon biochar (*Andropogon gayanus* Kunth cv. Planaltina). *Environ. Sci. Pollut. R.*, **26**, 33294-33303. <https://doi.org/10.1007/s11356-019-06463-6>
- Pusceddu, E. (2017) Comparison between ancient and fresh biochar samples, a study on the recalcitrance of carbonaceous structures during soil incubation. *Int. J. new Technol. Res.*, **3**, 39-46.

- Resta, B., Gaiardelli, P., Pinto, R., Dotti, S. (2016) Enhancing environmental management in the textile sector: An Organisational-Life Cycle Assessment approach. *J. clean prod.*, **135**, 620-632. <https://doi.org/10.1016/j.jclepro.2016.06.135>
- Rolland, L., Molle, P., Liénard, A., Bouteldja, F., Grasmick, A. (2009) Influence of the physical and mechanical characteristics of sands on the hydraulic and biological behaviors of sand filters. *Desalination.*, **248**, 998-1007. <https://doi.org/10.1016/j.desal.2008.10.016>
- Rosa, J.M., Garcia, V.S.G., Boiani, N.F., Melo, C.G., Pereira, M.C.C., Borrelly, S.I. (2019) Toxicity and environmental impacts approached in the dyeing of polyamide, polyester and cotton knits. *J. Environ. Chem. Eng.*, **7**, 102973. <https://doi.org/10.1016/j.jece.2019.102973>
- Sadezky, A., Muckenhuber, H., Grothe H., Niessner, R., Pöschl, U. (2005) Raman microspectroscopy of soot and related carbonaceous materials: Spectral analysis and structural information. *Carbon*, **43**(8), 1731-1742. <https://doi.org/10.1016/j.carbon.2005.02.018>
- Sahoo, T.R., Prelot, B. (2020) Chapter 7 - Adsorption processes for the removal of contaminants from wastewater: the perspective role of nanomaterials and nanotechnology. in: Bonelli, B., Freyria, F.S., Rossetti, I., Sethi, R. (Eds.). *Nanomaterials for the Detection and Removal of Wastewater Pollutants*. Elsevier, 161-222.
- Shee, A., Onyari, J., Jn, W., Munga, D. (2014) Methylene Blue Adsorption onto Coconut husks/Poly lactide Blended Films: Equilibrium and Kinetic Studies. *Chemistry and Materials Research*, **6**, 28-37.
- Sheng, C., 2007. Char structure characterised by Raman spectroscopy and its correlations with combustion reactivity. *Fuel*. **86**, 2316-2324. <https://doi.org/10.1016/j.fuel.2007.01.029>
- Shikuku, V.O., Jemutai-Kimosop, S. (2020) Efficient Removal of Sulfamethoxazole onto Sugarcane Bagasse-derived Biochar: Two and Three-parameter Isotherms, Kinetics and Thermodynamics. *J South African Journal of Chemistry*. *S. Afr. J. Chem.*, **73**, 111-119. <https://doi.org/10.17159/0379-4350/2020/v73a16>
- Suwunwong, T., Hussain, N., Chantrapromma, S., Phoungthong, K. (2020) Facile synthesis of corncob biochar via in-house modified pyrolysis for removal of methylene blue in wastewater. *Mater. Res. Express.*, **7**, 015518. <https://doi.org/10.1088/2053-1591/ab6767>
- Tomczyk, A., Sokołowska, Z., Boguta, P. (2020) Biomass type effect on biochar surface characteristic and adsorption capacity relative to silver and copper. *Fuel.*, **278**, 118168. <https://doi.org/10.1016/j.fuel.2020.118168>
- Torrens, A., Molle, P., Boutin, C., Salgot, M. (2009) Impact of design and operation variables on the performance of vertical-flow constructed wetlands and intermittent sand filters treating pond effluent. *Water Res.*, **43**, 1851-1858. <https://doi.org/10.1016/j.watres.2009.01.023>
- Tsaneva, V.N., Kwapinski, W., Teng, X., Glowacki, B.A. (2014) Assessment of the structural evolution of carbons from microwave plasma natural gas reforming and biomass pyrolysis using Raman spectroscopy. *Carbon.*, **80**, 617-628. <https://doi.org/10.1016/j.carbon.2014.09.005>
- Tosun, I. (2012) Ammonium Removal from Aqueous Solutions by Clinoptilolite: Determination of Isotherm and Thermodynamic Parameters and Comparison of Kinetics by the Double Exponential Model and Conventional Kinetic Models. *Int. J. Environ. Res. Public Health.*, **9**, 970-984. <https://doi.org/10.3390/ijerph9030970>
- Wang, G., Zhang, J., Chang, W., Li, R., Li, Y., Wang, C. (2018) Structural features and gasification reactivity of biomass chars pyrolyzed in different atmospheres at high temperature. *Energy*, **147**, 25-35. <https://doi.org/10.1016/j.energy.2018.01.025>
- Wu, J., Yang, J., Feng, P., Huang, G., Xu, C., Lin, B. (2019) High-efficiency removal of dyes from wastewater by fully recycling litchi peel biochar. *Chemosphere*, **246**, 125734. <https://doi.org/10.1016/j.chemosphere.2019.125734>
- Yaseen, D.A., Scholz, M. (2019) Textile dye wastewater characteristics and constituents of synthetic effluents: a critical review. *Int. J. new Technol. Res.*, **16**, 1193-1226. <https://doi.org/10.1007/s13762-018-2130-z>
- Yu, J., Sun, L., Berruoco, C., Fidalgo, B., Paterson, N., Millan, M. (2018) Influence of temperature and particle size on structural characteristics of chars from Beechwood pyrolysis. *J. Anal. Appl. Pyrol.* <https://doi.org/10.1016/j.jaap.2018.01.018>



- Zazycki, M.A., Borba, P.A., Silva, R.N.F., Peres, E.C., Perondi, D., Collazzo, G.C., Dotto, G.L. (2019) Chitin derived biochar as an alternative adsorbent to treat colored effluents containing methyl violet dye. *Adv. Powder Technol.*, **30**, 1494-1503. <https://doi.org/10.1016/j.apt.2019.04.026>
- Zhu, Y., Yi, B., Yuan, Q., Wu, Y., Wang, M., Yan, S. (2018) Removal of methylene blue from aqueous solution by cattle manure-derived low temperature biochar. *RSC Adv.*, **8**, 19917-19929. <https://doi.org/10.1039/C8RA03018A>